Contents

Vol. 67, No. 3, 2012

Simultaneous English language translation of the journal is available from Pleiades Publishing, Ltd.
Distributed worldwide by Springer. *Astrophysical Bulletin* ISSN 1990-3413.

ISSN 1990-3413, Astrophysical Bulletin, 2012, Vol. 67, No. 3, pp. 245–255. © Pleiades Publishing, Ltd., 2012.
Original Russian Text © O.K. Sil'chenko, V.L. Afanasiev, 2012, published in Astrofizicheskii Byulleten, 2012, Vol. 67, No. 3, pp. –.

Synchronous Evolution of Galaxies in Groups: NGC 524 Group

O. K. Sil'chenko[1]* and V. L. Afanasiev[2]

[1]*Sternberg State Astronomical Institute, Moscow State University, Moscow, 119991 Russia*
[2]*Special Astrophysical Observatory RAS, Russian Academy of Sciences, Nizhnii Arkhyz, 369167 Russia*

Received February 16, 2012; in final form, May 20, 2012

Abstract—With the means of panoramic spectroscopy at the SAO RAS BTA telescope, we investigated the properties of stellar populations in the central regions of five early-type galaxies—the NGC 524 group members. The evolution of the central regions of galaxies looks synchronized: the average age of stars in the bulges of all the five galaxies lies in the range of 3–6 Gyr. Four of the five galaxies revealed synchronized bursts of star formation in the nuclei 1–2 Gyr ago. The only galaxy, in which the ages of stellar population in the nucleus and in the bulge coincide (i.e. the nuclear burst of star formation did not take place) is NGC 502, the farthest from the center of the group of all the galaxies studied.

DOI: 10.1134/S1990341312030017

Key words: *galaxies: nuclei—galaxies: bulges—galaxies: stellar content—galaxies: evolution—galaxies: groups: individual: NGC 524*

1. INTRODUCTION

Most of the galaxies in the nearby Universe are group members: according to recent estimates [1], 54% of all the galaxies within 40 Mpc from us are clustered in groups with four or more members, and if we add the pairs and triplets, the number of galaxies in small groups raises to 82%. If we consider their properties: an obligatory presence of nearby gravitating "neighbors", and low, about 100 km/s, velocities of mutual passages (transits???) of galaxies, the characteristic dynamic crossing times of the entire space of the group several times shorter than the Hubble time, the groups are indeed the best place for the implementation of the so-called external secular evolution of galaxies (for the classification of the evolution mechanisms of galaxies—see the survey by Kormendy and Kennikat [2]). This implies the external effects, both gravitational and gas dynamic play an important, perhaps even dominant role in the evolution of galaxies in groups, in the construction of stellar subsystems of these galaxies. These effects can dramatically change the structure of galaxies, up to their morphological transformation.

The galaxies of the group are affected by the total gravitational potential of the group in which they move, and the common environment (hot intergalactic gas, if present in the group). Then, it seems likely that the reconstruction of the global structure and, in particular, the formation of central stellar subsystems in them may be synchronized, i.e. the average age of stellar populations in the centers of galaxies is one and the same. Almost all the mechanisms of the gravitational (tidal) interaction, as well as a number of gas dynamic mechanisms (frontal pressure, static compression by the hot medium) lead to the concentration of gas of the disk galaxy at its center, followed by the subsequent starburst with the formation of the secondary stellar population in the nucleus and bulge of the galaxy. The discovery of synchronization in the evolution of central galactic regions in groups could be a significant argument in favor of the dominant role of external effects, and the lack thereof, on the contrary, should attract attention to the differences of initial conditions in the evolution of galaxies.

More than ten years ago we took up the study of stellar populations in central regions of galaxies in groups with the MPFS and BTA of the Special Astrophysical Observatory of the Russian Academy of Sciences (SAO RAS). We managed to investigate 2–3 central galaxies in six nearby groups. In Leo I [3], and in the NGC 5576 [4] and NGC 3169 [5] groups of galaxies the properties of stellar population in the circumnuclear disks of large galaxies turned out to be the same. The last stars there have formed relatively recently, 1–3 Gyr ago, in spite of the early type of the host galaxies, and in the Leo I group the circumnuclear stellar disks even have the same spatial orientation. In the Leo triplet (NGC 3623/NGC 3627/NGC 3628), on the contrary, the age of the stellar population and the kinematics of gas in the centers of NGC 3623, and

*E-mail: olga@sai.msu.su

Table 1. Global parameters of the studied galaxies

Galaxy	NGC 502	NGC 509	NGC 516	NGC 518	NGC 532
Morphological type (NED)	$SA0^0(r)$	S0?	S0	Sa:	Sab?
R_{25}, arcsec (RC3) [16]	34	43	39	52	75
B_T^0 (RC3) [16]	13.57	14.20	13.97	13.56	12.91
M_B (RC3+NED)	−18.3	−17.7	−17.9	−18.3	−19.0
V_r, km/s (NED)	2489	2274	2451	2725	2361
Separation from group center, kpc [16],[17]	282	151	68	101	126
Distance to group, Mpc [18]	24				
Photometric bulge parameters according to [23]					
$r_{\rm eff}$, arcsec	3.5	2.9	2.9	7.4	5.4
$n_{\rm Sersic}$	1.5	1.5	1.85	2	2
Kinematic bulge parameters according to the present paper					
$V_{\rm rot}(r_{\rm eff})$, km/s	62 ± 11	18 ± 15	26 ± 9	68 ± 20	27 ± 15
$\sigma_*(r_{\rm eff})$, km/s	94 ± 3	77 ± 13	65 ± 6	100 ± 12	110 ± 8

NGC 3627 are significantly different [6]. We hence concluded that the galaxies of the triplet have gathered into a single group only recently, less than 1 Gyr ago. In the Leo II group, where unlike in the previous groups mentioned, the gas, emitting in X-rays was detected in two central galaxies, the observed circumnuclear kinematically decoupled stellar structures turned out to be old. They have different ages of formation—6 and 10 Gyr for NGC 3608, and NGC 3607, respectively [7]. At the same time, the peripheral lenticular galaxies NGC 3599, and NGC 3626 reveal the formation (current star formation) of central stellar subsystems [8]. The evolution of the central regions of early-type galaxies in the rich massive group NGC 80 also turned out to be asynchronous. This group as well has a noticeable X-ray halo [9] both in the nuclei and in the central spheroids, the estimates of the average age of stellar populations are ranging from 1.5–3 Gyr (in the E-galaxy NGC 83 and S0-galaxy IC 1548) to more than 10 Gyr in NGC 79 (elliptical) and IC 1541 (lenticular galaxy).

This paper will present the results of analysis of the properties of stellar population in the galaxies of another massive group with X-ray-emitting gas: the NGC 524 group. This group was cataloged for the first time by Geller and Khuchra in 1983 [10]. Then, only 8 member galaxies were listed in it. Later, Yan Vennik [11] has visually inspected the Palomar maps and found 18 bright and 13 dwarf galaxies there via the interaction hierarchy method. In the latest catalogs Brough et al. [12], applying the FOF (friend-of-my-friend) method have identified 16 members in the NGC 524 group, and, according to the Catalog of Nearby Groups of Makarov and Karachentsev [1] the group is also attributed with 16 member galaxies. If we adopt the radius of the group from the catalog by Makarov and Karachentsev, $R_h = 391$ kpc, the NED extragalactic database discovers in this group 10 galaxies brighter than $M_B \sim -16$. Most of the bright members of the group are classified as lenticular galaxies. Given the galaxy velocity dispersion in the group of about 150–190 km/s [1, 12], the group is rather massive, $1.7 \times 10^{13}\, M_\odot$ [13]. The ROSAT satellite was mapping the X-ray-emitting gas in the NGC 524 group, however, the radius of the X-ray spot is less than 60 kpc, hence in some papers the hot gas is not considered to belong to the halo of the group, but only to the central galaxy NGC 524 [14]. Using the method of panoramic spectroscopy we have investigated the stellar population and the kinematics of circumnuclear regions of the brightest non-central galaxies of the groups: NGC 502, NGC 509, NGC 516 (all lenticular), NGC 518 and NGC 532 (spiral galaxies of early types). The global characteristics of the studied galaxies, adopted from the NED and HYPERLEDA databases are given in Table 1. For the central galaxy of the group, NGC 524, the results, obtained with the MPFS/BTA have been published earlier [15].

2. OBSERVATIONS AND DATA PROCESSING

For the central parts of five largest galaxies of the NGC 524 group the data were obtained via the panoramic spectroscopy method using the Multi-Pupil Fiber Spectrograph (MPFS) in the primary focus of the 6-m BTA telescope of the SAO RAS (see the description of the instrument in [19]). To study the stellar populations and stellar kinematics the blue-green spectral range 4150–5650 Å with reverse dispersion 0.75 Å per pixel was recorded (spectral resolution of about 3 Å). For the galaxy with a rich emission spectrum (with a large amount of ionized gas in the center), NGC 532, we also obtained the spectrum in the red range 5800–7200 Å to investigate the kinematics of the gas component in the center of the galaxy, and using the equivalent width of the Hα emission line to calculate the correction to the Lick Hβ index for the distortion of the absorption line by emission. The detector used was a EEV 42-40 CCD, 2048×2048 pixels. At the observations with the MPFS, an array of square microlenses, assembled in a square field of view sized 16×16 elements constructs a matrix of micro-pupils, which is then reformed into a pseudo-slit via the optical fibers and fed to the spectrograph input. This configuration allows to simultaneously record 256 spectra, each of which characterizes a spatial element of the image of the galaxy sized about $1''.0 \times 1''.0$. To calibrate the wavelength scale each time before and after the object, a comparison spectrum of the helium-neon-argon lamp was exposed; in order to correct for the vignetting and different transmissions of microlenses, we used the inbuilt lamp of the spectrograph and the spectrum of the dawn sky. The initial data processing, which includes the bias subtraction (the electronic zero), removal of traces of cosmic particles, extraction of one-dimensional spectra for each pixel, and linearization of the selected spectra was performed using a set of programs written in the IDL software environment.

To calculate the kinematic parameters of the stellar component—radial velocity and stellar velocity dispersion at this point—the spectrum of each spatial element after the continuum subtraction and the transformation to the velocity scale was subjected to cross-correlation with the spectra of type G8–K2 giants. They were observed the same night and using the same instruments as the galaxy. For the cross-correlation of young stellar populations we used the dawn sky (G2 class) as the reference range. The accuracy of the wavelength scales and the zero point of measured velocities were monitored by the night sky line [O I] λ5577 Å. We estimate the accuracy of individual measurements of radial velocities of the stellar component as 5–7 km/s. Having obtained the kinematic parameters for analyzing the properties of stellar populations—the age, total metallicity and the ratio of the abundances of magnesium (the α-process element) and iron—we calculated the Lick Hβ, Mgb, Fe5270 and Fe5335 indices for each individual spectrum. Determination of the Lick system was taken from the publications of Worthey et al. [20, 21]. The resulting maps of the Lick indices—Mgb and $\langle \mathrm{Fe} \rangle \equiv (\mathrm{Fe5270} + \mathrm{Fe5335})/2$ for all galaxies and Hβ for the lenticular galaxies without a noticeable emission component in the spectra are presented in Figs. 1–5. Detailed model calculations exist for these strong absorption lines within the stellar population synthesis (SPS) models, which associate the indices (equivalent widths of absorption lines) with the mean (weighted with the luminosity of stars) properties of the stellar populations, the so-called SSP-equivalent (Simple Stellar Population) ages and metallicities. From the variety of available model calculations for the comparison with our results we have chosen the Thomas et al. models [22], since these models are calculated for several values of the magnesium-to-iron abundance ratio, and, therefore, can also determine, besides the age and total metallicity, this third parameter of the stellar population as well.

Table 2. Spectral observations with MPFS

Galaxy	Date	T(exp), min	Range, Å	Seeing, arcsec
NGC 502	17.09.2006	60	4150–5650	2.0
NGC 509	18.09.2006	120	4150–5650	1.5
NGC 516	17.09.2006	60	4150–5650	2.0
NGC 518	19.08.2007	150	4150–5650	1.3
NGC 532	08.10.2004	120	4150–5650	1.2
NGC 532	06.09.2008	40	5800–7300	1.5

A detailed log of observations of the NGC 524 group of galaxies is presented in Table 2.

3. RESULTS

3.1. Two-Dimensional Distributions of Lick Indices

The morphology of the panoramic distribution of the properties of stellar population in central regions of galaxies can be qualitatively evaluated by the distributions of the Lick indices of metallicity and hydrogen. These distributions are presented in Figs. 1–5. Consider the individual features of these distributions for each galaxy.

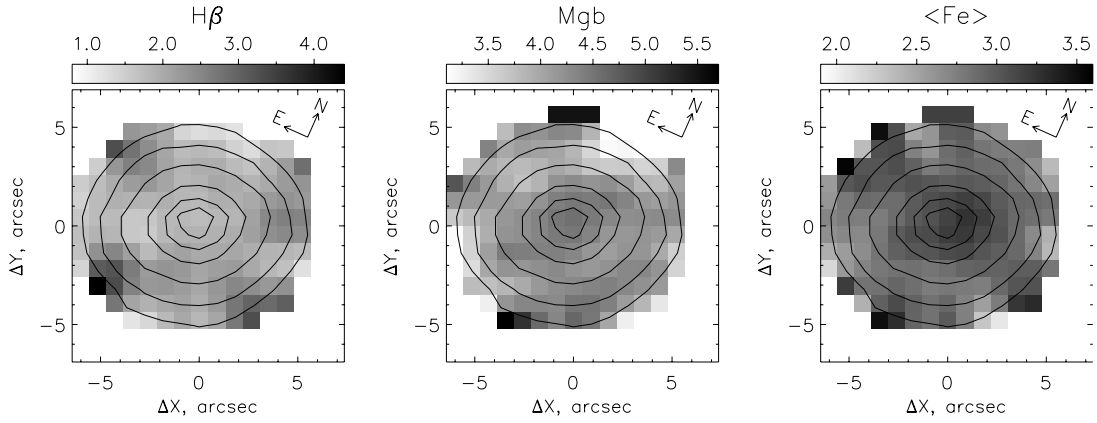

Fig. 1. The maps of the Lick indices Hβ, Mgb, $\langle$Fe$\rangle \equiv$ (Fe5270 + Fe5335)/2 for the central region of NGC 502. The isophotes show the distribution of surface brightness in the green (λ 5000 Å) continuum.

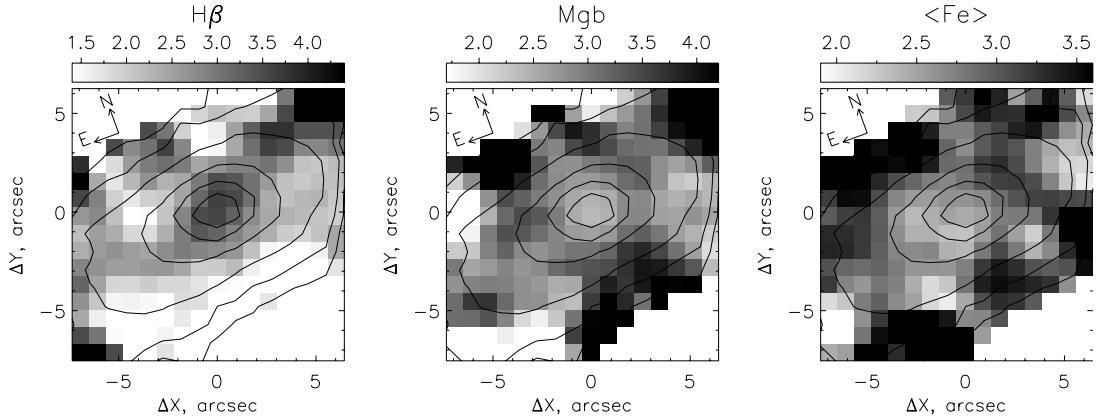

Fig. 2. The maps of the Lick indices Hβ, Mgb, $\langle$Fe$\rangle \equiv$ (Fe5270 + Fe5335)/2 for the central region of NGC 509. The isophotes show the distribution of surface brightness in the green (λ 5000 Å) continuum.

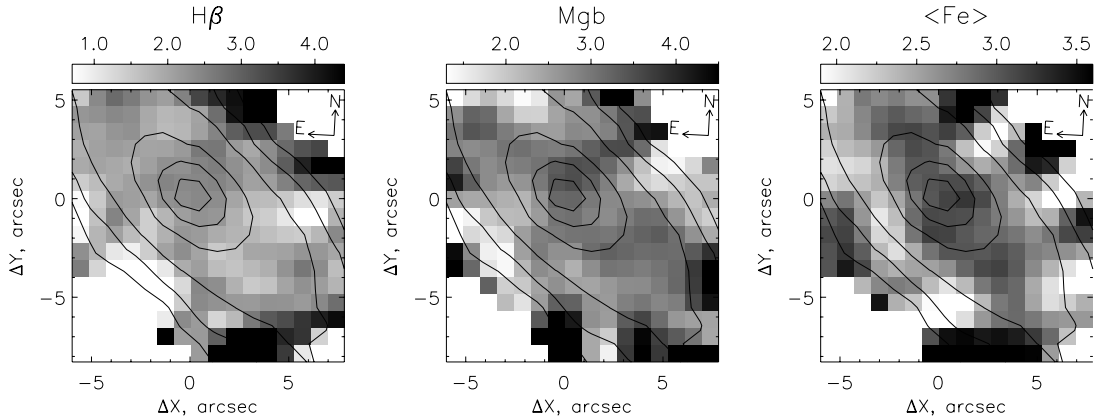

Fig. 3. The maps of the Lick indices Hβ, Mgb, $\langle$Fe$\rangle \equiv$ (Fe5270 + Fe5335)/2 for the central region of NGC 516. The isophotes show the distribution of surface brightness in the green (λ 5000 Å) continuum.

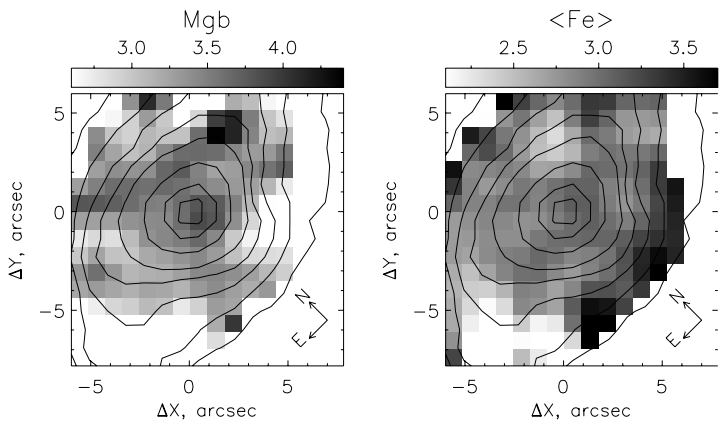

Fig. 4. The maps of the Lick indices Mgb and $\langle \mathrm{Fe} \rangle \equiv (\mathrm{Fe5270} + \mathrm{Fe5335})/2$ for the central region of NGC 518. The isophotes show the distribution of surface brightness in the green (λ 5000 Å) continuum.

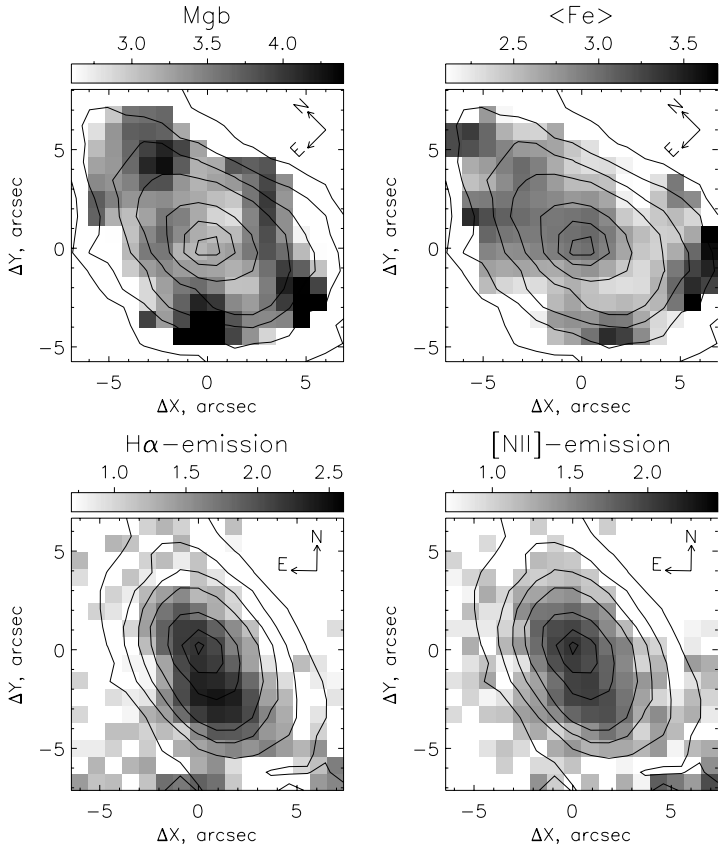

Fig. 5. The maps of the Lick indices Mgb and $\langle \mathrm{Fe} \rangle \equiv (\mathrm{Fe5270} + \mathrm{Fe5335})/2$ (top plot) and the logarithms of fluxes in the Hα and [N II] λ 6583 Å emission lines in arbitrary units (bottom plot) for the central region of NGC 532. The isophotes show the distribution of surface brightness in the green (λ 5000 Å)(upper row) and red (λ 6500 Å) (bottom row) continuum.

NGC 502, Fig. 1. The maps of the Lick indices for NGC 502 can be characterized by an increase of equivalent line widths of magnesium and iron in the nucleus with a simultaneous weakening of Hβ. This can be interpreted as an enhanced metallicity of stars in the geometric center of the galaxy: the galaxy revealed a chemically decoupled nucleus. In other respects, no notable features or anisotropy are observed in the distributions: NGC 502 is visible almost face-on, the properties of the stellar population are centrally symmetric, including the center of the galaxy.

NGC 509, Fig. 2. This lenticular galaxy, visible edge-on, exhibits an opposite feature of the distribution of Lick indices: one can note a sharp peak of Hβ in the nucleus, a less pronounced enhancement of the hydrogen index near the equatorial plane of the galaxy, as well as compact minima of the magnesium and iron indices near the centers of the isophotes. We will see below that this mainly reflects the effect of age: the stellar population in the nucleus is much younger than around the nucleus. Interestingly, the Mgb minimum is surrounded by a regular circular ring of increased index values, although the isophotes are extended considerably stronger. It justifies the averaging of the indices in round rings in the estimates of the stellar population parameters in the bulge.

NGC 516, Fig. 3. NGC 516 is also a small lenticular galaxy like NGC 509, and as well visible edge-on. It is located very close to the center of the group, only about 70 kpc projected onto the picture plane of the central galaxy NGC 524, and their radial velocities are close. In Fig. 3, just like in the case of NGC 509, we observe the strengthening of the Hβ index in the nucleus, but this time the indices of magnesium and iron exhibit the minima instead of the maxima at this region. Moreover, an increase of the iron indices clearly has a disk morphology: these are not compact spots, but rather the narrow lanes across the entire field of view. If the strengthening of Hβ is the effect of age (as we shall see below), we can assume that the burst of star formation in NGC 516 lasted longer than that in the center of NGC 509, that the star formation did not take place in the nucleus, but rather in the disk, and the stellar disk managed to get enriched with heavy elements during this burst.

NGC 518, Fig. 4. The spiral galaxy NGC 518 is visible at a large angle to the line of sight, but not exactly edge-on [23]. The spectra of the central region inside the profile of the Hβ absorption line reveal a moderate emission, hence in this case in Fig. 4 we do not give the map of distribution of the Lick Hβ index. Before using it to analyze the properties of stellar population, it has to be corrected for the contribution of the emission. A chemically decoupled nucleus of the galaxy can be distinguished in the distributions of the magnesium and iron indices; it is possibly compact only in Mgb, and has an extended shape in the iron index. We repeatedly encountered this feature at the centers of early-type galaxies (e.g., in the S0-galaxy NGC 1023 [24]). It can be interpreted as a rapid completion of the burst of star formation in the nucleus and a subsequent continuous process of star formation in the circumnuclear ring.

NGC 532, Fig. 5. In the central region of this galaxy the emission lines of ionized gas are very strong. To properly take them into account, we took a panoramic spectrum in the red range, and in Fig. 5, besides the maps of Lick indices of magnesium and iron (equivalent widths of absorption lines), we additionally present the maps of flux distribution in the Hα and [N II] λ6583 emission lines (in arbitrary counts). All the distributions look complex and asymmetrical, even the maps of flux distributions in the emission lines. The peak of emission of the forbidden nitrogen line comes from the nucleus, whereas the maximum of the Hα emission line—from a compact region of about 4″ south of the nucleus. From the flux ratio in these lines (Hα/[N II] = 1.66 in the nucleus, Hα/[N II] $\approx$ 2 outside the nucleus), using the diagnostics by Veilleux and Osterbrock [25], we can say that the nucleus of NGC 532 is a LINER, and the major part of current star formation is localized in the circumnuclear disk, and exactly to the south of the nucleus. The measured emission line intensities and the character of excitation of the ionized gas we have determined, is used later on to correct the Lick Hβ index for the distortion by emission.

3.2. Age and Chemical Composition of Stellar Population in Galactic Nuclei and Bulges

Taking advantage of the panoramic spectroscopy, we summarized the spectra in the rings, centered at the nuclei of galaxies, moving along the radius with at increments of 1″. This allowed to obtain the total spectra for the galaxy bulges with the same signal-to-noise ratio, as in the nucleus. At our exposures and after the summation of the spectra in the rings, the accuracy of measured indices is about 0.1 Å, which was determined by us in the survey of lenticular galaxies with the MPFS by repeated observations of some galaxies [26]. Next, we discuss the characteristics of stellar populations in the nuclei and in the ring zones of the bulges, obtained from the Lick indices.

To determine the average (weighted with the luminosity of stars) characteristics of the stellar population: the age, total metallicity, the ratio of the abundances of magnesium and iron, let us compare our measurements of the Lick indices in the galaxies with the calculations from [22], made in the framework of the SSP (Simple Stellar Population)

model, that is, assuming the same age and the same chemical composition in all stars that contribute to the integral spectrum (of one spatial element of the galaxy in our case). To determine the ratio of the abundances of magnesium and iron, we will use a diagram that maps the Mgb and ⟨Fe⟩ indices. To determine the age and total metallicity we compare the Hβ hydrogen index and a composite index of metals $[\mathrm{MgFe}] \equiv (\mathrm{Mgb}\,\langle\mathrm{Fe}\rangle)^{1/2}$: this diagram allows to separate the effects of age and metallicity (remove the degeneracy), since the line series of equal metallicity and equal age have different slopes and form a kind of a curvilinear coordinate grid, which allows to determine both the age and metallicity of stellar population based on the position of the observational point on the diagram. The Hβ index, which is used to determine the age of the stellar population should be corrected for the contribution of the emission component. In the case of NGC 532, for which we possess a spectrum in the red range, this was done by the equivalent width of the Hα emission line. In the nucleus, we used the average ratio of the equivalent widths of the Balmer emission lines $\mathrm{EW}(\mathrm{H}\beta) = 0.25\,\mathrm{EW}(\mathrm{H}\alpha)$, found from a large mixed sample of spiral galaxies by Stasinska and Sodre [27]. At a distance of 4–6″ from the nucleus, dominated by current star formation, instead of 0.25 we used a coupling (clustering???) coefficient of 0.35, typical of gas excitation by young stars [28]. If we use the relation from Stasinska and Sodre [27] for the bulge, the age estimate in the bulge would decrease by 0.5 Gyr—from 4 to 3.5 Gyr. For NGC 518, where the emission lines are weaker than in NGC 532, and there exist no data in the red spectral range, we used a statistical mean ratio for the early-type galaxies $\mathrm{EW}(\mathrm{H}\beta) = 0.6\,\mathrm{EW}([\mathrm{O\,III}]\ \lambda 5007\ \text{Å})$ [29]. The calculated in such a way equivalent width of the Hβ emission line is the correction to be added to the measured Hβ index, to correct it for the emission (by the definition of the Lick indices as the equivalent widths).

Table 3 gives the Lick indices and the stellar population parameters, derived from them for the nuclei of studied galaxies. Figure 6 demonstrates a comparison of the observed indices with the models from [22]. The first thing that catches the eye is that in four out of five galaxies, the stellar nuclei are very young, with an average age of the stellar population of 1–2 Gyr. Secondly, in four out of five galaxies (though not the same) the metallicity of stellar population in the nuclei is very high, with the total metal abundance 3–5 times higher than solar. Obviously, we see the consequences of the recent highly efficient bursts of star formation in the nucleus, and the chemically decoupled nuclei of galaxies they generated. The magnesium-to-iron ratio in three out of four young nuclei is solar, and only in NGC 518, where we noted a larger compactness of the magnesium index peak compared with that of iron on the Lick index maps (Fig. 4), this ratio is one and a half times greater than solar. This means that in these three nuclei the burst of star formation has been long enough, lasting at least 2–3 Gyr. It was shorter in the nucleus of NGC 518, though it was going on for the same 2–3 Gyr in the immediate vicinity of the nucleus, already starting from the radius of 2″ (300 pc).

Table 3. Lick indices and parameters of stellar population in the nuclei

Galaxy	Hβ	Mgb	⟨Fe⟩	T, Gyr	[Z/H]	[Mg/Fe]
NGC 502	1.83	4.60	3.29	3.5	+0.6	+0.13
NGC 509	3.99	1.85	2.00	1	0.0	0.0
NGC 516	2.49	3.08	3.00	1.5	+0.4	0.0
NGC 518	2.36	3.86	2.84	2	+0.6	+0.17
NGC 532	3.07	3.19	2.99	1	$> +0.7$	0.0

Table 4. Lick indices and parameters of stellar population in the bulges

Galaxy	Hβ	Mgb	⟨Fe⟩	T, Gyr	[Z/H]	[Mg/Fe]
NGC 502	1.95	4.13	2.82	4	+0.3	+0.19
NGC 509	1.90	3.06	3.02	5	+0.1	−0.13
NGC 516	1.96	2.65	2.84	6	−0.1	−0.19
NGC 518	2.23	3.12	2.78	3	+0.1	0.0
NGC 532	2.06	3.42	2.68	4	+0.1	+0.10

Table 4 lists the Lick indices and the stellar population parameters, derived from them for the bulges of studied galaxies, taken as the integral in the rings of 4″–6″ (0.65–1.0 kpc) radius. Figure 7 compares these data with the models from [22]. The scatter of the magnesium and iron abundance ratio in the stellar populations of the bulge is significant: it may be either higher than solar (in the bulge of NGC 502), or significantly lower than solar, as in the bulges of NGC 509 and NGC 516. If $[\mathrm{Mg/Fe}] > 0$ is typical for the spheroids of a sufficiently large mass [30, 31], $[\mathrm{Mg/Fe}] < 0$ is on the other hand very rarely found among the galaxies, and mainly in dwarfs. The chemical evolution specialists interpret the overabundance of iron relative to magnesium as a sign of the flare

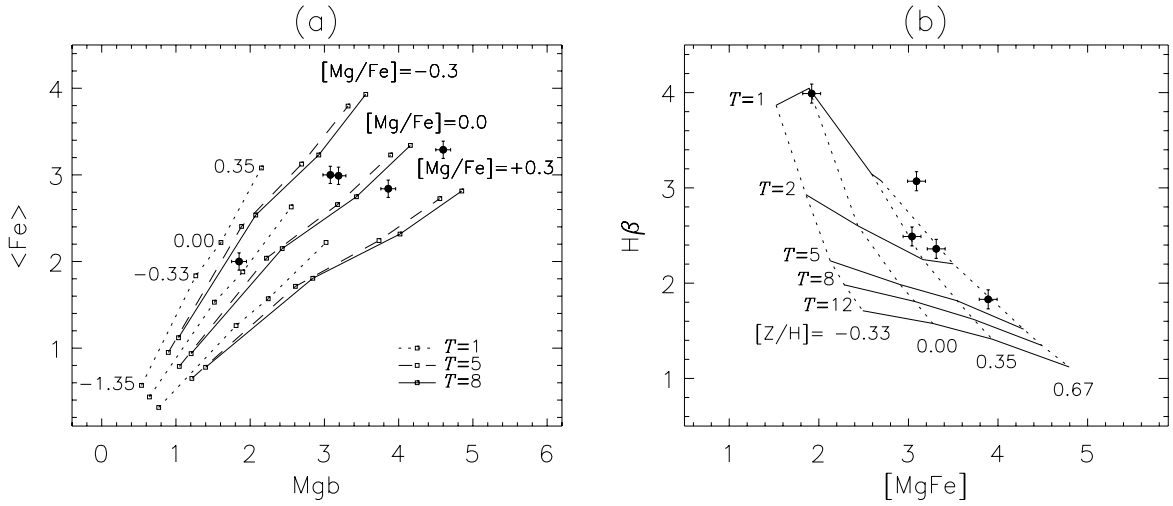

Fig. 6. The diagnostic "index–index" diagrams for the measurements of the nuclei of five "non-central" galaxies from the NGC 524 group (black dots with error bars). Small icons, connected by different lines at the left plot and solid lines at the right plot is the calculation according to the model of stellar populations of the same age [22]; the age of the models is given in gigayears (Gyr). The total metallicity of the models for [Mg/Fe] = 0.0 is marked next to the model check points (frames of reference???), indicated by small signs on the left and connected by dashed lines on the right.

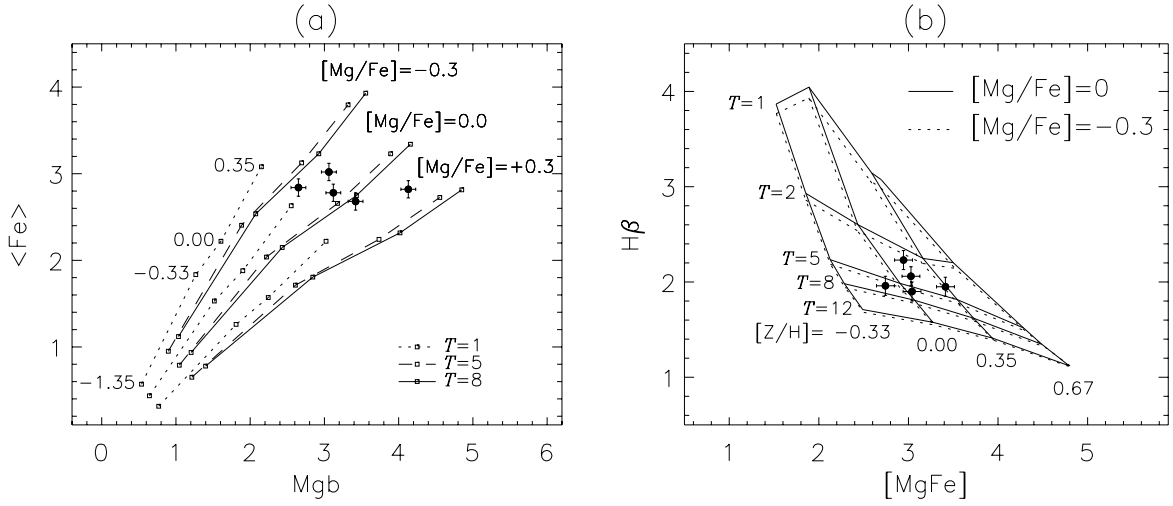

Fig. 7. The diagnostic "index–index" diagrams for the measurements in the bulges (the rings of the 4–6″ radius) for the five "non-central" galaxies of the NGC 524 group (black dots with error bars). The model sequences are similar to those shown in Fig. 6. The diagnostic Hβ–[MgFe] diagrams use models with a different magnesium to iron ratio: solid line—[Mg/Fe] = 0.0, and dashed line—[Mg/Fe] = −0.3.

history of star formation history with a small number of bursts separated by long intervals of time, lasting at least 2–3 Gyr [32]. Meanwhile, the average age of stars in all the five bulges of the NGC 524 group of galaxies is enclosed in a fairly narrow range of values, of about 3–5 Gyr, if for NGC 509 and NGC 516 we use the models from [22] with the deficiency of magnesium relative to iron (Fig. 7b).

The accuracy of finding the ages of stellar populations for the bulges of five studied galaxies is about 1 Gyr given the galaxy age of 3–4 Gyr, and about 2 Gyr at the age of 5–6 Gyr. This means that the bulges of all the five studied galaxies have approximately the same average age of stellar population within the measurement accuracy.

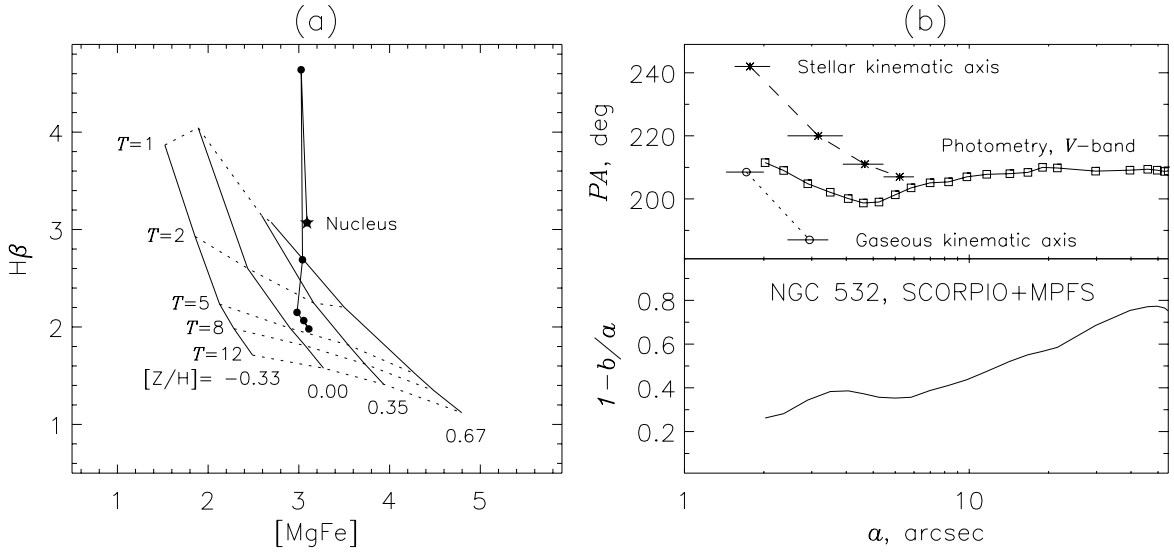

Fig. 8. The circumnuclear ring in NGC 532: (a) the diagnostic diagram Hβ–[MgFe] for the measurements in the nucleus (asterisk) and in the rings, starting at $R = 2''$, and further at a step of $1''$ (black dots), model sequences—as in Figs. 6b and 7b; (b) results of the isophote image analysis of NGC 532 in the V-band [23]; the top panel compares the orientation of the major axis of the isophotes and the direction of the kinematic major axes (the direction of the maximal radial velocity gradient) for the ionized gas and stars according to the data of the panoramic spectroscopy with the MPFS, and the bottom plot shows the variation in the isophote ellipticity.

3.3. Relic Circumnuclear Star Formation Rings

In addition to the bulges and unresolved nuclei—two separate stellar systems that were found to have substantially different star formation histories in most of the galaxies studied—we can also note such structures as relict circumnuclear rings of star formation, that were earlier under way. As we already noted, in NGC 518, 300 pc from the center the iron index abruptly climbs with the monotonic decrease of the magnesium index—the Mg/Fe ratio in the nucleus and its vicinity varies roughly by one and a half. This can be interpreted as a longer star formation in the ring compared with a short burst in the geometric center of the galaxy. However, in NGC 518, this difference in the duration of star formation is visible only in the chemical composition of stars and is not revealed in the estimates of the average age of stellar populations. The average age of stars in NGC 518 gradually increases from 2 to 3 Gyr along the radius. In NGC 532, the circumnuclear ring of recent star formation can be seen with "naked eye"(???). Figure 8a shows the Hβ–[MgFe] diagram for NGC 532: the azimuthally averaged measurements of the Lick indices along the radius of the galaxy, starting from the nucleus, further in the ring $R = 2''$ and then in one second of arc. It can be seen how with the distance from the nucleus the age of the stellar population first drops by a few hundred million years, and then abruptly increases, while in the bulge at the distances from the center of 0.6–1.0 kpc it practically does not vary. We can see that the youngest stellar population in the center of NGC 532 is concentrated in the ring of the $R = 2''$ radius. The most curious is that this ring is isolated both photometrically and kinematically. Figure 8b shows the variation along the radius of orientation of the major isophote axis in the V-band (calculated and published by us [23]) compared with the central kinematic major axes, determined from the velocity fields of stars and ionized gas; the bottom plot shows the variation along the isophote ellipticity radius. The $R = 2''$ radius is photometrically decoupled: at this radius, the ellipticity of the isophotes is maximal, and the major axes of the stellar component, both photometric and kinematic, simultaneously turn to larger position angles. Since the kinematic major axis of the stellar component is turned in the same direction as the photometric major axis, we can interpret the extended structure in the center of NGC 532 as an inclined circumnuclear stellar disk, which was formed, according to the Lick indices, rather recently, within 1 Gyr from our epoch.

4. CONCLUSIONS AND DISCUSSION

We investigated the properties of stellar populations in the central regions of five largest galaxies of the NGC 524 group via the method of panoramic spectroscopy, using the multi-pupil spectrograph,

mounted at the prime focus of the BTA. The centermost galaxy of the group, a giant S0 NGC 524 was investigated by us using the same instruments earlier. We diagnosed there a homogeneous old ($T > 10$ Gyr) stellar population in all its structural components—in the nucleus, the bulge and in the multilayered large-scale disk [15, 33]. In contrast with the central galaxy, the other galaxies of the group, as it turned out, have intermediate-age populations in the bulge and young stellar populations in the chemically decoupled stellar nuclei. Interestingly, the average age of the stellar populations in the bulges is about the same in all the five galaxies, it amounts to $T_{SSP} \approx 3$–5 Gyr, and the average age of the stellar nuclei is approximately equal in four of the five galaxies studied: $T_{SSP} \approx 1$–2 Gyr. Only the S0-galaxy NGC 502, farthermost from the group center did not undergo a separate burst of star formation in the nucleus: its nucleus and bulge have the same age of 4 Gyr.

Such a synchronous evolution of galaxies in the group points to the defining role of environment in stimulating the inner events in the lives of galaxies, in the first place, the bursts of star formation in their centers. In the NGC 524 group, no hot gaseous environment is present over the entire volume of the group. However, a compact X-ray halo was registered only around the NGC 524 itself. It is therefore evident that the gravitational interactions play the defining role here. The time scales of the build-up /superstructure (???надстройки центральных областей галактик) of the central regions of galaxies that we have identified for the NGC 524 group, fall within the modern cosmological calculations of the hierarchical clustering of matter in the Universe. Indeed, in modern cosmological models, massive clusters of galaxies, $M > 10^{13} M_{\odot}$, become gravitationally bound near the redshift $z = 1$. For example, in a recent paper [34] the first "companions" (non-central galaxies of the group) cross the virial radius at the redshift of $z = 1.5$ (9 Gyr ago) and the more recent of the large galaxies—around $z = 0.7$ (6 Gyr ago). Falling into the volume of the virial radius, the galaxies experience the gravitational influence of both the potential of the entire group [35], and the tidal effects from the other group members in close encounters(approaches?? близкие сближения) [36]. These gravitational interactions breach the axial symmetry of the galactic disks, accreted by the group, leading to the formation of bars, and the bars, in turn, redistribute the gas in the disks, forcing it to accumulate in the centers of galaxies. Further on, the bars may dissolve under the gravitational effect of the central concentration of mass. As a result, massive bursts of star formation are expected exactly is in the central kiloparsec, which should lead to the growth of bulges (and a decrease of the average age of the bulge stars), while in the galaxies that have not had the bulges before—just to the formation of central spheroidal components, or pseudobulges. Indeed, at $z = 0.4 - 0.7$ in a dense environment of clusters and groups the blue disk galaxies are dominating [37, 38], which a great many mistake for the spiral galaxies that are only approaching their transformation into the S0s. In effect, these may be the disc galaxies including the S0s, that are in the process of a vigorous build-up of the bulge immediately after the accretion into a dense environment [39]. This process halts at $z < 0.4$, which is 3–4 Gyr ago, what is consistent with the bulge ages found by us in the disk galaxies of the NGC 524 group. Further, in 1–2 Gyr the galactic nuclei host the secondary bursts of star formation, more compact, and obviously more modest in the consequences than those that were building-up the bulges. Interestingly, they are also synchronized. They are likely to be related with the dynamic evolution of the group, whose crossing time is approximately 2–3 Gyr. Around the large galaxies of the NGC 524 group we have discovered a significant number of blue dwarf galaxies, obviously rich in gas [23]. A passage of a large galaxy through the center of the group may possibly provoke a massive fall-out (выпадение ???) of dwarf companions on it, and this would supply the matter for a nuclear burst of star formation, which is quickly and efficiently burnt out (small lenticular galaxies NGC 516 and NGC 509, where we found young stellar nuclei, are completely swept-out of gas, according to [17]).

ACKNOWLEDGMENTS

This work was supported by the Ministry of Education and Science of Russian Federation (state contracts no. 16.552.11.7028 and 16.518.11.7073). We thank A. V. Moiseev and A. A. Smirnova for the observational support with the MPFS. We have used the Lyon-Meudon Extragalactic Database (LEDA), maintained by the LEDA team of the CRAL at the Lyon Observatory (France), and the NASA/IPAC (NED) database of extragalactic data, managed by the Jet Propulsion Laboratory at Caltech under the state contract with the National Aeronautics and Space Administration (USA). This work was supported by RFBR grant no. 10-02-00062a.

REFERENCES

1. D. Makarov and I. Karachentsev, Monthly Notices Roy. Astronom. Soc. **412**, 2498 (2011).
2. J. Kormendy and R. C. Kennicutt Jr., Annu. Rev. Astronom. Astrophys. **42**, 603 (2004).
3. O. K. Sil'chenko, A. V. Moiseev, V. L. Afanasiev, et al., Astrophys. J. **591**, 185 (2003).

4. O. K. Sil'chenko, V. L. Afanasiev, V. H. Chavushyan, and J. R. Valdes, Astrophys. J. **577**, 668 (2002).
5. O. K. Sil'chenko and V. L. Afanasiev, Astron. Lett. **32**, 534 (2006).
6. V. L. Afanasiev and O. K. Sil'chenko, Astronom. and Astrophys. **429**, 825 (2005).
7. V. L. Afanasiev and O. K. Sil'chenko, Astron. and Astrophys. Trans. **26**, 311 (2007).
8. O. K. Sil'chenko, A. V. Moiseev, and A. P. Shulga, Astronom. J. **140**, 1462 (2010).
9. O. K. Sil'chenko and V. L. Afanasiev, Astron. Rep. **52**, 875 (2008).
10. M. J. Geller and J. P. Huchra, Astrophys. J. Suppl. **52**, 61 (1983).
11. J. Vennik, Baltic Astronomy **1**, 415 (1992).
12. S. Brough, D. A. Forbes, V. A. Kilborn, and W. Couch, Monthly Notices Roy. Astronom. Soc. **370**, 1223 (2006).
13. D. A. Forbes, T. Ponman, F. Pearce, et al., Publ. of the Astron. Soc. of Australia **23**, 38 (2006).
14. J. Osmond and T. Ponman, Monthly Notices Roy. Astronom. Soc. **350**, 1511 (2004).
15. O. K. Sil'chenko, Astronom. J. **120**, 741 (2000).
16. G. de Vaucouleurs, A. de Vaucouleurs, H. G. Corwin Jr., et al., *Third Reference Catalogue of Bright Galaxies. Volume I: Explanations and References* (New York, Springer, 1991).
17. Ch. Sengupta and R. Balasubramanyam, Monthly Notices Roy. Astronom. Soc. **369**, 360 (2006).
18. J. L. Tonry, A. Dressler, J. P. Blakeslee, et al., Astrophys. J. **546**, 681 (2001).
19. V. L. Afanasiev, S. N. Dodonov, and A. V. Moiseev, in *Proc. Conf. Stellar Dynamics: from Classic to Modern,* Ed. by L. P. Osipkov and I. I. Nikiforov (St. Petersburg Univ. Press, 2001), p. 103.
20. G. Worthey, S. M. Faber, J. J. Gonzàlez, and D. Burstein, Astrophys. J. Suppl. **94**, 687 (1994).
21. L. A. Jones and G. Worthey, Astrophys. J. **446**, L31 (1995).
22. D. Thomas, C. Maraston, and R. Bender, Monthly Notices Roy. Astronom. Soc. **339**, 897 (2003).
23. M. A. Ilyina and O. K. Sil'chenko, Astron. Rep. (in press).
24. O. K. Sil'chenko, Astronom. J. **117**, 2725 (1999).
25. S. Veilleux and D. E. Osterbrock, Astrophys. J. Suppl. **63**, 295 (1987).
26. O. K. Sil'chenko, Astrophys. J. **641**, 229 (2006).
27. G. Stasinska and I. Sodre Jr., Astronom. and Astrophys. **374**, 919 (2001).
28. D. E. Osterbrock, *Astrophysics of Gaseous Nebulae and Active Galactic Nuclei* (Mill Valley, CA: Univ. Science Books, 1989).
29. S. C. Trager, S. M. Faber, G. Worthey, and J. J. Gonzàlez, Astronom. J. **119**, 1645 (2000).
30. G. Worthey, S. M. Faber, and J. J. Gonzàlez, Astrophys. J. **398**, 69 (1992).
31. S. C. Trager, S. M. Faber, G. Worthey, and J. J. Gonzàlez, Astronom. J. **120**, 165 (2000).
32. G. Gilmore and R. F. G. Wyse, Astrophys. J. **367**, L55 (1991).
33. O. K. Sil'chenko, I. S. Proshina, A. P. Shulga, and S. E. Koposov, Monthly Notices Roy. Astronom. Soc. submitted (2012).
34. T. Kaufmann, L. Mayer, M. Carollo, and R. Feldmann, submitted to Monthly Notices Roy. Astronom. Soc.; arXiv:1201.6605 (2012).
35. A. Villalobos, G. De Lucia, S. Borgani, and G. Murante, Monthly Notices Roy. Astronom. Soc. (in press); arXiv:1202.0550 (2012).
36. K. Bekki and W. J. Couch, Monthly Notices Roy. Astronom. Soc. **415**, 1783 (2011).
37. D. J. Wilman, A. Oemler, Jr., J. S. Mulchaey, et al., Astrophys. J. **692**, 298 (2009).
38. D. W. Just, D. Zaritsky, D. J. Sand, et al., Astrophys. J. **711**, 192 (2010).
39. D. Burstein, L. C. Ho, J. P. Huchra, and L. M. Macri, Astrophys. J. **621**, 246 (2005).